Developing Analogs for Magnetic Synapses

Gabriela Gonzalez Magana, McNair Scholar
The Pennsylvania State University

McNair Faculty Research Adviser:
Paris Von Lockette, Ph.D.
Associate Professor of Mechanical Engineering
Department of Engineering
College of Engineering
The Pennsylvania State University

Introduction

Human brain could easily recognize different objects since it processes sensory and motor signals in parallel. The brain has many neural pathways that can replicate functions to correct small brain changes in development or temporary loss of function through damage [1]. The ability to overcome these changes in development is the result of the neuroplasticity. These changes range from individual neurons making new connections, to systematic adjustments like cortical remapping. The junction between the neuron's circuits, synapses, are the place to look for neuroplasticity. Synapses dominate the architecture of the brain and are responsible for the massive parallelism. Therefore, researchers are currently seeking engineered material analogs for the particular responses exhibited by biological neuromorphic materials. Neuromorphic systems, which mimic the nervous system in the brain, have recently become known as strong candidates to overcome the technical limitations owing to their proficiency in cognitive [2]. To successfully implement these neuromorphic systems, it is important to research and develop artificial synapses capable of synapse functions.

In the beginning neuromorphic computing was described as a concept involving large integrated electronics analogs systems that mimic biological neural networks. Therefore, a great importance for hardware implementation of the neuromorphic computation systems has been the realization of physical devices with synaptic functions. The first devices to emulate synaptic functions were complementary metal oxide semiconductor (CMOS) neuromorphic circuits [3]. However, the performance of these CMOS circuits is hard to scale up to a size comparable with the brain and is limited to access external memory. This has engendered motivation to explore bio-inspired neuromorphic systems focusing in resistive switching memory and memristors. Memristors have gained the spotlight because of their desirable characteristics as artificial synapses including device speed, small footprint, low energy consumption and analog switching [4]. Learning more about neuromorphic systems will allow us to create simulations that allow us to test brain injury treatments to help recover from trauma brain. Also, these simulations may help us develop sensors using electrical components such as memristors whose resistance relies on how much charge has passed through it in the past, mimics the way calcium ions behave at the junction between two neurons in the human brain where the junction is known as a synapse.

For example, environmental enrichment is the key to develop new connections that relies on sensory stimuli. However, in order to develop these new connections, it is important to understand electronic responses and brain functions that will help simulate the human brain in a technological way. One such response is the hysteresis in input versus output signals.

Hysteresis is a common phenomenon in physical systems and occurs when the system's output depends not only on its present inputs but also on past inputs, basically, when the system exhibits memory. Development of engineered neuromorphic materials focuses on creating materials that exhibit such memory. One possible model material involves arrays of rotating magnetic particles suspended in a medium. As the particle spin particles are placed in a rotating magnetic field. This generally assures the effective dipole moment, which permits the formulation of torque expressions for spherical shells. The work seeks to development simulations of spinning magnetic particles in a visco-elastic medium as a simulation framework for exploring hysteresis response in a similarly-structured engineered neuromorphic material.

1. Background/Literature Review

1.1 Brain plasticity

Researchers interested in understanding the factors that can change brain circuits investigate the behaviors of brain plasticity which is the change in neural circuitry. Brain plasticity or memory of response, is what the brain uses to store memories and process information. Without this ability, the brain would be unable to develop from infancy through to adulthood or recover from brain injury [1]. The Brain function relies on circuits of spiking neurons with synapses playing the key role of merging transmission with memory storage and processing.

Brain plasticity refers to the capacity of the nervous system to change its structure and its function over a lifetime, in reaction to environmental diversity. Neural plasticity, allows neurons to regenerate both anatomically as well as functionally, and to form new synaptic connections. Therefore, the best place to look for plasticity changes is at synapses which are the junction between the neurons. This is called Synaptic plasticity. Synaptic plasticity is the ability of synapses to reconfigure the strength with which they connect two neurons according to the past electrical activity of these neurons. It represents one of the most fundamental and important functions of the brain. In hardware, artificial synapses endowed with plasticity allow neural networks to learn and adapt to a changing environment. A very enduring form of synaptic plasticity is called long-term potentiation (LTP) a synaptic enhancement that follows brief, high-frequency electrical stimulation in the hippocampus and neocortex. Brain plasticity, or neuroplasticity, is the ability for the brain to recover and restructure itself. This adaptive potential of the nervous system allows the brain to recover after disorders or injuries.

The following image illustrates signs of synaptic plasticity emerging in a living brain.

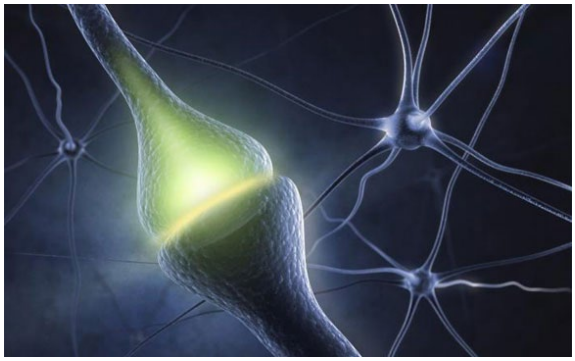

Figure 1: Signs of synaptic plasticity emerging in a living brain by Sukbin Lim (Neuroscience, 2015)

The lighting in the image shows how the living brain accomplishes the feat of beholding and recognizing stimuli. The lighting represents signs of synaptic plasticity emerging in a living brain while it accomplishes the feat of beholding and recognizing stimuli. These synapses are studied experimentally by stimulating the fiber tract. By studying the synaptic plasticity, we better understand the connections of the human brain and the way those functions can be simulated in artificial synapses. Developing simulations of those artificial synapses are the goals of this work.

1.2 Memristors responses in hysteresis

According to previous studies memristors are considered as the best solution to imitate the performance of synapses plasticity [8]. Since memristors cover a gap in the capabilities of basic electronic components by remembering the history of the applied electric potentials, and are considered to bring neuromorphic computers closer. A memristor is a passive two-terminal circuit element in which the resistance is a function of the history of the current through and voltage across the device. In other words, memristors are Nano scale devices with a variable resistance and the ability to remember their resistance when power is off. Memristors are based on the history of applied electrical stimuli. These capabilities lead to analog switching, which resembles biological synapses where the strength can increase or decrease depending on the applied action potential.

The nonlinear behavior of a memristor is shown in Figure 2, This shows evidences of the results of an intricate resistance versus the voltage of a memristor.

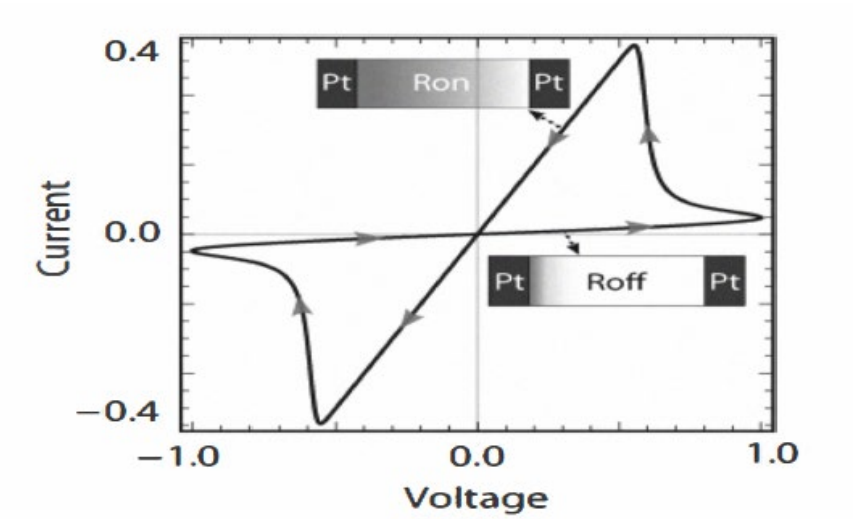

Figure 2: Nonlinear behavior of memristor (Chakraverty M. and Kittur M.H 2012)

The hysteresis loop pinched at the origin of the V – I characteristic is the well-known fingerprint of the memristor excited by sinusoidal signal. The pinching at the origin in Fig. 2 occurs because both current (I) and voltage (V) become zero at the same time. In order to show that hysteresis is at the origin (I, V) = (0, 0), calculations on the memristance must be determine. Different approaches have been done in previous studies; for example, in one of the studies the researchers treated the two-terminal circuit of the memristor as the time integral of the element's current I(t) and voltage V(t). However, in this research we will use the concept of the memristor to investigate if we can use rotating magnetic particles to produce a similar hysteresis response in the applied field versus magnetization.

1.3 Magnetic field and Magnetic particles

Previous research has focused on soft and hard magnetic particles such as Iron and Bromine, embedded in the elastomer matrix to produce magnetorheological elastomers (MREs). Soft magnetic particles have no preferred magnetic orientation, when exposed to a uniform magnetic field **H** will have magnetization, **M**, aligned with the external field. Hard-magnetic particles with remanent magnetization $\boldsymbol{M_{rem}}$ will ideally have **M** remain aligned with the axis of $\boldsymbol{M_{rem}}$ which is local to the particle and thus allows for the generation of magnetic torque **T**. Figures 3a and 3b shows a representation of soft and hard magnetic particles orientations.

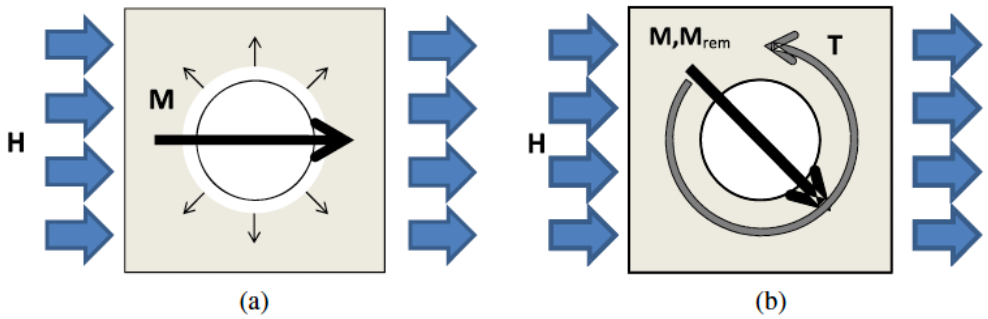

(a) (b)

Figure 3 (a). Orientation of soft-magnetic particle and Figure 3(b). Orientation of hard-magnetic particle (P von Lockette et al 2011 Smart Mater. Struct. 20 105022)

According to classical electromechanics, for soft-magnetic particles magnetization **M** of a particle remains parallel to the external magnetic field **H.** Therefore, there is not net force or torque acting on spherical particle with respect to that field if it is uniform. In contrast to soft-magnetics particles, hard-magnetics particles generate substantial torques. Since, in this research we are developing system of equations for magnetic torques acting on anisotropic body to form neuromorphic systems, we focus on both hard-magnetic particles and soft-magnetic particles to produce hysteresis responses in the applied field versus magnetization. The magnetic torque **T**, within the particles themselves is determined by the cross product of the magnetization and the magnetic field **T** = **M** x **H**. However, since soft-magnetic particles are not driven by magnetic torques acting on individual particles this magnetic particle rely on demagnetizing effects to provide a restoring force, e.g. the particle themselves must be geometrically anisotropic.

Electric or magnetic fields are useful for manipulating dispersions containing polarizable dielectric and paramagnetic colloids and nanoparticles. Magnetic or electric fields can be used for rotation, however, magnetic fields are more common in experiments because their effects on the dispersion are easier to control, as electric fields can generate unwanted currents, electroosmotic flows, and electrochemical reactions [11]. Therefore, in this study we focused on magnetic fields to create our system of equations. Based on previous studies, to control how strong mutual polarization among particles is relative to the polarization due solely to the external field $\boldsymbol{H_0}$, the magnetic of the susceptibility $|\chi|$ was used.

2. Methods

Consider a bar rotating in plane as shown in Figure 1. The bar can be magnetized by an external field, H. Once magnetized, the bar develops an internal magnetization M. It is important to realize that we can determine the amount of our external field, H, acting along $x - y$ axes *separately* from how we determine the amount of magnetization parallel and perpendicular to the bar itself. These are the next steps in our analysis:

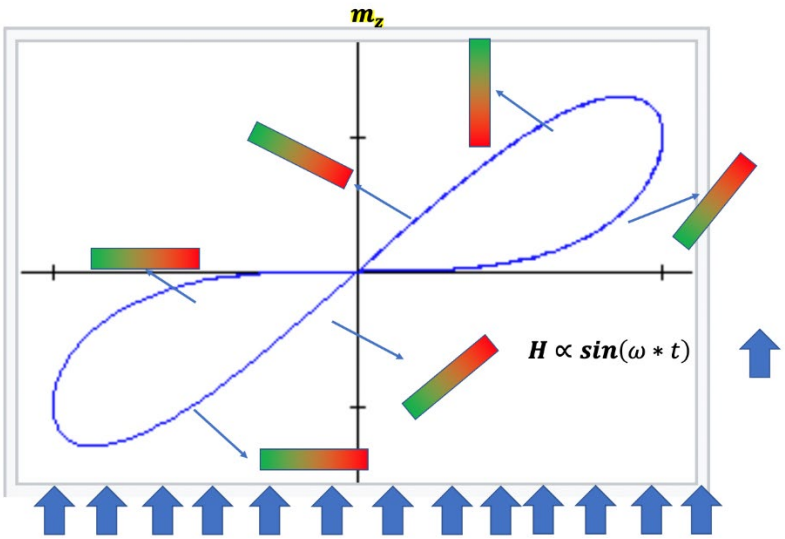

Figure 1. Bar rotating in a magnetic field showing the polarized body in the field

To begin we first define the rotation matrix, ***A*.** This matrix will be used to calculate the internal Magnetization, ***M*. *A*** is represented as

$$\boldsymbol{A} = \begin{bmatrix} cos\theta & -sin\theta \\ sin\theta & cos\theta \end{bmatrix}$$

were θ is the deflection angle of the parallel and perpendicular component directions of the magnetic field ***H*** and magnetization ***M*** as shown in Figure 2.

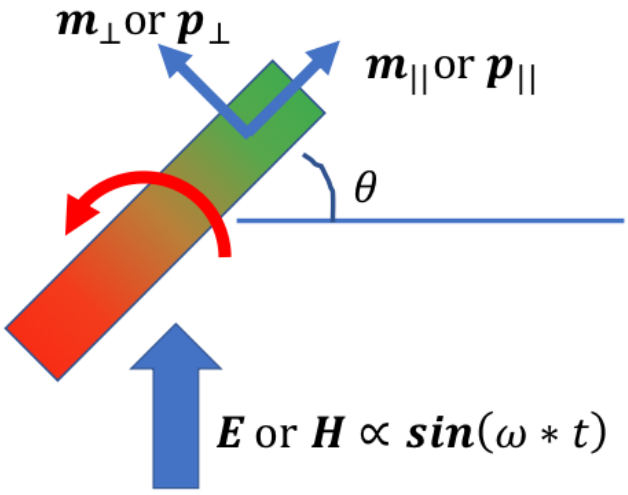

Figure 2. Schematic showing the angle deflection

Next, let m be represented as two vectors parallel and perpendicular to the bar

$$\boldsymbol{m} = \boldsymbol{m}_{||} + \boldsymbol{m}_{\perp} \tag{1}$$

and subsequently

$$\boldsymbol{m} = m_{||}\,\widehat{\boldsymbol{m}}_{||} + m_{\perp}\widehat{\boldsymbol{m}}_{\perp} \tag{2}$$

where $\left\|\boldsymbol{m}_{||}\right\| = m_{||}$ and $\|\boldsymbol{m}_{\perp}\| = m_{\perp}$. Next, we define the direction vectors perpendicular and parallel to the bars, $\widehat{\boldsymbol{m}_{||}}$ and $\widehat{\boldsymbol{m}_{\perp}}$, respectively, in the x – y coordinate system as

$$\widehat{\boldsymbol{m}}_{||} = \cos\theta\ \ \boldsymbol{i} + \sin\theta\ \ \boldsymbol{j} \tag{3}$$

and

$$\widehat{\boldsymbol{m}}_{\perp} = -\sin\theta\ \ \boldsymbol{i} + \cos\theta\ \boldsymbol{j} \tag{4}$$

with θ defined in Figure 1. This allows us by substitution to write

$$\boldsymbol{m} = [m_{\parallel}\cos\theta - m_{\perp}\ \sin\theta]\boldsymbol{i} + \ [m_{\parallel}\sin\theta + m_{\perp}\ \cos\theta]\boldsymbol{j}$$

In eq. (5), $m_{||}$ and $m_{\perp}$ must be derived from demagnetization factors associated with the geometry of the bar. From reference [5] we find for an oscillating field of frequency ω and magnitude H_0 that

$$m_{||} = \chi * \sin(\theta) * H_0 sin(\omega t) \tag{5}$$

is the component of magnetization parallel to the bar and

$$m_{\perp} = \frac{\chi}{\chi+1} * \cos(\theta) * H_0\ sin(\omega t) \tag{6}$$

is the component perpendicular to the bar. Again, by substitution we can write

$$\boldsymbol{m} = \left(\chi * \sin(\theta) * \widehat{\boldsymbol{m}}_{||} + \frac{\chi}{\chi+1} * \cos(\theta) * \widehat{\boldsymbol{m}}_{\perp}\right) H_0 sin(\omega t)$$

which gives the results in a coordinate system attached to the bar. This may be recast in the x – y coordinate system by substitution of eq. (3) and (4) to give our final result

$$\boldsymbol{m} = \Big(\chi * \sin(\theta) * [\cos\theta\ \ \boldsymbol{i} + \sin\theta\ \ \boldsymbol{j}]\ + \frac{\chi}{\chi+1} * \cos(\theta) * [-\sin\theta\ \ \boldsymbol{i} + \cos\theta\ \boldsymbol{j}]\ \Big) H_0 sin(\omega t)$$

In eq. (7) we have assumed

$$\boldsymbol{H} = \begin{bmatrix} 0 \\ H_0 \end{bmatrix} sin(\omega t) \tag{7}$$

in the x – y coordinate system. H_0 is the amplitude of the magnetic field.

After $\boldsymbol{m}$ is calculated we used its results to calculate the Torque, $\boldsymbol{T}$, where Torque is

$$\boldsymbol{T} = \boldsymbol{m} \times \boldsymbol{H} \tag{8}$$

and ϕ is the direction of the magnetic field.

Deriving torque from external field we obtain

$$\boldsymbol{T} = \boldsymbol{T_{EM}} + \boldsymbol{T_{viscous}} + \boldsymbol{T_{drag}} + \boldsymbol{T_{viscoelastic}}$$

where $\boldsymbol{T_{EM}}$ is the driving torque from external field, $\boldsymbol{T_{viscous}}$ is the retarding torque from viscous-elastic response.

where eq. (8) can be derived as

$$J\theta'' = \sum T \ \ (in\ plane) \tag{9}$$

and $\boldsymbol{J}$ is the polar moment of inertia. $\sum \boldsymbol{T} \ \ (in\ plane)$ is derived for rotational drag coefficient and its viscosity factors which give us the following form of a second order non-linear differential equation

$$J\theta'' = -D_\omega \theta' - D_\theta \theta + H_0 \cos\theta$$

D_ω is the rotational drag coefficient, which contains the viscosity, D_θ is the spring like a drag term in our equation, and in eq. (11)

We can recast variables as follows without loss of generality,

$$c_1 = \frac{D_\omega}{J} \tag{10}$$

$$c_2 = -\frac{D_\theta}{J} \tag{11}$$

$$c_3 = \frac{H_0}{J} \tag{12}$$

To obtain:

$$\theta'' = -C_1 \theta' - C_2 \theta + C_3 \cos\theta \tag{13}$$

where C_1 is the ratio of rotational drag coefficient over polar moment of inertia, $C_2$is the spring-like drag term over polar moment of inertia and C_3 represents the strength of the magnetic field with respect to the polar moment of inertia.

We use the derived differential equation of eqs. (14-17) to measure the damping ratio and measure how oscillations in a system decay after a disturbance. We investigate if we can use an aggregate of rotating magnetic particles to produce a hysteresis response in the applied field versus magnetization.

The damping ratio is denoted by ζ and it is calculated as

$$\zeta = \frac{C_1}{2\sqrt{C_2}} \tag{14}$$

where

$$\zeta = \frac{Actual\ Damping}{Critical\ Damping} \tag{15}$$

and

$$Actual\ Damping = \frac{D_\omega}{J} \tag{16}$$

and

$$Critical\ Damping = 2\sqrt{\frac{D_\theta}{J}} \tag{17}$$

3. Results of Damping Ratio Visual Simulations

1. Constant Magnetic field with varying damping ratios (Zeta)

The results of the derived differential equation and damping ratio were used to create and examine visualized simulations in MATLAB. These simulations are similar spring-mass system with a difference of adding a steady stream of air pushing the mass, in other words we are adding torque to our system. As mentioned, the damping ratio measures how oscillations in a system decay after a disturbance and find the equilibrium position. The equilibrium position is the balance of the spring force and whatever torque has been applied.

Figure 1.3 shows the effect of varying damping ratios, ζ, of the derived second order differential equation with constant magnetic field of one. As the damping ratio varied, different oscillation cases were observed: undamped, underdamped, and overdamped. Undamped occurred when $\zeta = 0$, meaning there is not damping and we are getting perfect oscillation with a small rotation. Underdamped occurred when $\zeta < 1$. We can overshoot pass our equilibrium position, then oscillate back until the signal will settle down at its equilibrium position. Overdamped happens when $\zeta > 1$. This occurred due to the rotational drag coefficient term (D_ω) that acted on the velocity. If it D_ω is very high it takes longer to achieve equilibrium.

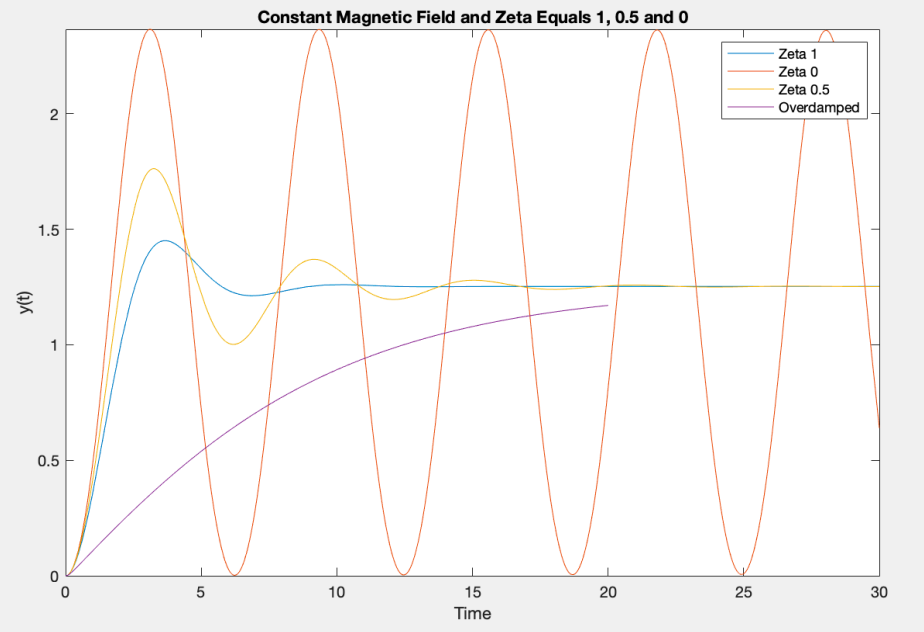

Figure 1.3 The effect of varying damping ratio of the second order system

2. *Change in Magnetic field with $\zeta = 1$) 1 and varying τ* where τ is the constant time

We used the same calculations as Figure 1.3, but for this case we only focused on $\zeta = 1$ with varying τ and H_0 . In Figures 1.4(a), (b) and (c), the magnetic field (Ho) sets the amplitude, the τ sets the period. We know that $period\ (T) = \frac{2\pi}{\omega}$ [6], therefore, in our calculations we let frequency ω be τ to set the period to be constant. We conclude that as Ho is larger, the rotation is larger, so as the torque rises and fall to higher and lower values the particle amplitude rotational amplitude increases.

In Figures 1.4a-c we have $\zeta = 1$and the Ho doubles and triples for each Figure, going from 2 to 4 and 2 to 6. The only thing that changes in each Figure is the τ. In Figure 1.4(a), 1.4(b) and 1.4(c) we have small, medium and large τ. As predicted the torque goes up as we increase Ho because the rotation is getting larger and the polar of inertia is getting smaller. Another observation from this Figures is that as τincreases the period is getting larger and the rotation is getting smaller meaning that the polar inertia is getting bigger and its harder to have the system spin.

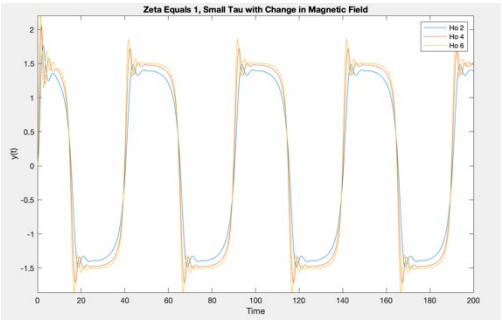

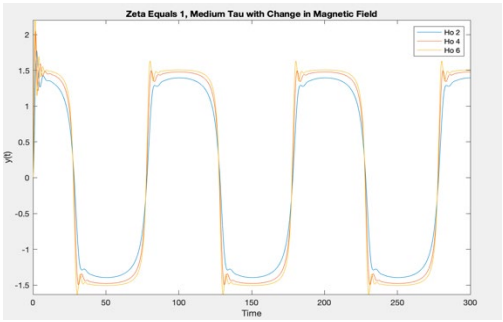

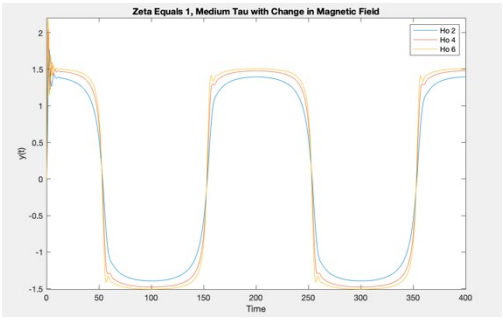

Small τ (a) **Medium τ (b)** **Large τ (c)**

Figure 1.4. The effect of varying magnetic field (Ho) on damping ratio equal 1 with (a) small τ, (b) medium τ, and large τ. As Ho increases, the rotation decreases and the period increases.

3. Change in Magnetic field with varying damping ratio $\zeta = 0.5$ and varying τ

The following Figures are similar to the Figures 1.4a-c, however, in these Figures we have Zeta equals to 0.5. In Figures 1.5a-c, as in In Figure 1.4a-c, we have 50, 100 and 200 τ. In contrast, the results in this figure shows that if we have a smaller damping ratio, we have more torque rising and falling to higher and lower values regardless the Ho. The rotation is the same as the simulation where the damping ratio is 1. Figures 1.5a, b and c have the same amplitudes in the first period. However, as τ increases the period increases and the rotation decreases, but there still a larger torque in the smaller damping ratio.

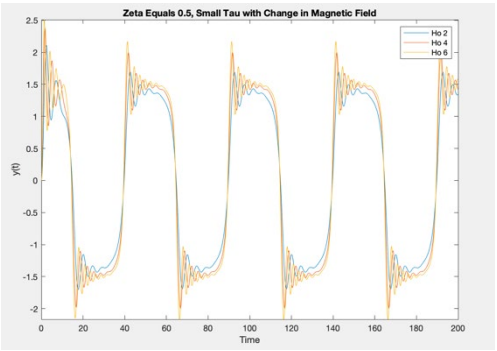

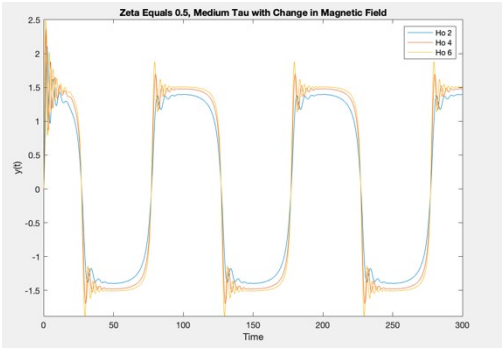

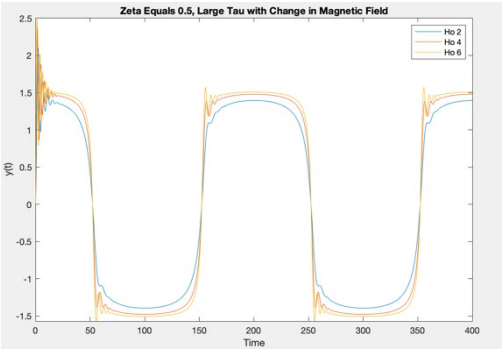

Small τ (a) **Medium τ (b)** **Large τ (c)**

Figure 1.5. The effect of varying magnetic field (Ho) on damping ratio $\zeta = 0.5$ with (a) small τ, (b) medium τ, and large τ. As Ho increases, the rotation still larger than zeta equals to 1 and the period still increases.

4. *Change in Magnetic field with varying damping ratio $\zeta = 0$ and varying τ*

As in the previous Figure, the Figures 1.6a-c have the same change in magnetic field and small, medium and large τ. The only difference from previous cases, is the damping ratio is 0 which shows there is not damping. In this case the system tries to follow the external signal but instead it oscillates. With small τ we start off at zero, the field swings down and up, but is moving slowly enough without damping that as it is moving down the bar is oscillating around at whatever direction the field pointing. It is interesting to note that in the case of large τ, the oscilating system takes more than one cycle to reach its apex at $y(t) \cong 4.5$ before reversing immediately achieve oscillations about $y(t) \cong +4.5$.

Even when we had a large period the bar is actually moving slowly, and it is oscillating in the similar line.

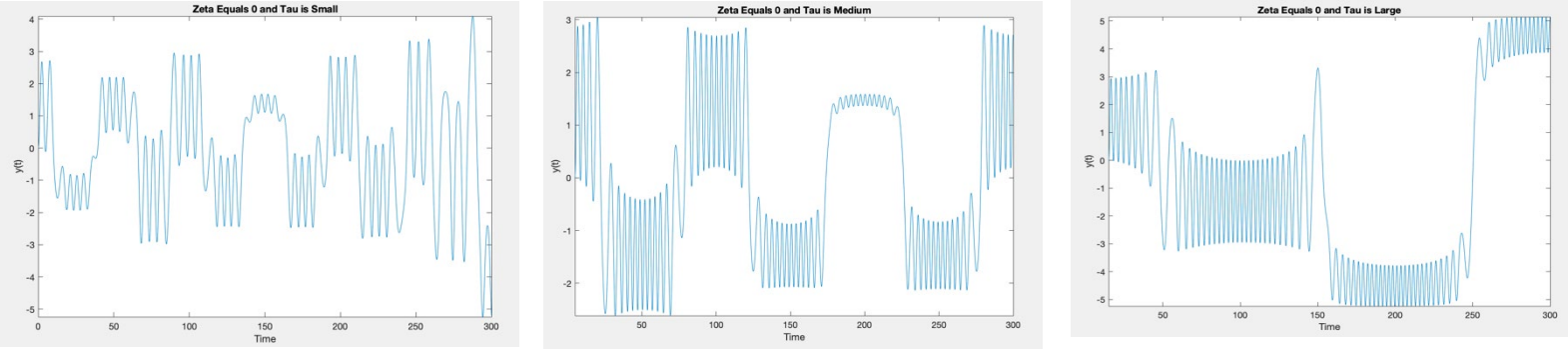

Small τ (a) **Medium τ (b)** **Large τ (c)**

Figures 1.6. The effect of varying magnetic field (Ho) on damping ratio (Zeta) equal 0 with (a) small τ, (b) medium τ, and large τ.

4. Conclusion

In this work, we study the material analogs for the particular responses exhibited by biological neuromorphic materials. We derived equations governing a rotating magnetic body that were similar to those governing a spring-mass system. A key difference was the inclusion of magnetic torque, which acted analogously to a stream of air pushing the mass. These simulations visualize the results from a unidirectional, sinusoidal magnetic field with proscribed amplitude and period; and with varying damping ratio of the system itself. After analyzing the simulations, we observed that for constant magnetic field, if the drag coefficient term D_ω is high it the system takes longer times to achieve its equilibrium position. For the change in magnetic field with varying damping ratio and varying period, we conclude that as the field amplitude is larger, the rotation amplitude is larger, so the torque rises and fall to higher and lower values. Finally, as the period increases the displacement amplitude decreases, showing that inertia is possibly a factor in the overshoot response.

References

1) Nelson, D. (2017). What an experimental control is and why it's so important. *Science Trends*. doi:10.31988/scitrends.4717
2) Sanghyeon Choi, Seonggil Ham and Gunuk Wang (March 29th 2019). Memristor Synapses for Neuromorphic Computing, Memristors - Circuits and Applications of Memristor Devices, Alex James, IntechOpen, DOI: 10.5772/intechopen.85301. Available from: https://www.intechopen.com/books/memristors-circuits-and-applications-of-memristor-devices/memristor-synapses-for-neuromorphic-computing
3) Kim, M. K., Park, Y., Kim, I. J., & Lee, J. S. (2020). Emerging Materials for Neuromorphic Devices and Systems. *IScience*, *23*(12), 101846. https://doi.org/10.1016/j.isci.2020.101846
4) Wang, R., Shi, T., Zhang, X., Wang, W., Wei, J., Lu, J., Zhao, X., Wu, Z., Cao, R., Long, S., Liu, Q., & Liu, M. (2018). Bipolar Analog Memristors as Artificial Synapses for Neuromorphic Computing. *Materials*, *11*(11), 2102. https://doi.org/10.3390/ma11112102
5) Lockette, P. . v. o. n., Lofland, S. E., Biggs, J., Roche, J., Mineroff, J., & Babcock, M. (2011b). Investigating new symmetry classes in magnetorheological elastomers: cantilever bending behavior. *Smart Materials and Structures*, *20*(10), 105022. https://doi.org/10.1088/0964-1726/20/10/105022
6) Deziel, Chris. "How to Calculate the Period of Motion in Physics" sciencing.com, https://sciencing.com/calculate-period-motion-physics-8366982.html. 19 April 2021.
7) M. Chakraverty and H. M. Kittur, "Evidence of hysteresis from first principle dft simulations of I–V curves in Pt/TiO2−x - TiO2/Pt memristive systems," *2012 International Conference on Devices, Circuits and Systems (ICDCS)*, Coimbatore, 2012, pp. 379-383, doi: 10.1109/ICDCSyst.2012.6188749.
8) Kamran Eshraghian, Kyoung-Rok Cho, Omid Kavehei, Soon-Ku Kang, Derek Abbott and Sung-Mo Steve Kang, Memristor MOS Content Addressable Memory (MCAM): Hybrid Architecture for Future High-Performance Search Engines, IEEE TRANSACTIONS ON VERY LARGE-SCALE INTEGRATION (VLSI) SYSTEMS (Accepted for Publication).
9) Gutchess, A. (2014). Plasticity of the aging brain: New directions in cognitive neuroscience. *Science*, *346*(6209), 579–582. https://doi.org/10.1126/science.1254604
10) Sukbin Lim, et al., “Inferring learning rules from distributions of firing rates in cortical neurons,” Nature Neuroscience, 2015; doi:10.1038/nn.4158
11) Lequeux, S. *et al*. A magnetic synapse: multilevel spin-torque memristor with perpendicular anisotropy. *Sci. Rep.* **6**, 31510; doi: 10.1038/srep31510 (2016).
12) Lockette, P. . v. o. n., Lofland, S. E., Biggs, J., Roche, J., Mineroff, J., & Babcock, M. (2011b). Investigating new symmetry classes in magnetorheological elastomers: cantilever bending behavior. *Smart Materials and Structures*, *20*(10), 105022. https://doi.org/10.1088/0964-1726/20/10/105022

13) Salikhov, K.M., Sagdeev, R.Z., & Buchachenko, A.L. Molin, Yu.N. (Ed.). (1984). Spin polarization and magnetic effects in radical reactions. Netherlands: Elsevier.